

Elemental Composition of Hyper-Metal-Poor Stars Formed in Dust-Enriched Dense Shells of Population III Supernova Remnants

Takaya Nozawa¹ (takaya.nozawa@ipmu.jp)

T. Kozasa², K. Nomoto¹, K. Maeda¹, N. Tominaga³, H. Umeda⁴

¹Kavli IPMU, University of Tokyo, ²Hokkaido University, ³Konan University, ⁴University of Tokyo



Abstract

Dust grains in the early universe are considered to be important agents to trigger the formation of low-mass stars in metal-poor environments (e.g., Omukai 2000; Schneider et al. 2003). The condition that the dust-induced fragmentation occurs depends on dust-to-gas mass ratio as well as size distribution of dust (Omukai et al. 2005; Schneider et al. 2006; 2012a; 2012b). We investigate the origin of dust grains in metal-poor star-forming clouds and the feasibility of the grain growth through accretion of refractory elements in the collapsing dense cores.

In Nozawa et al. (2007), we found that a fraction of dust grains formed in the ejecta of Pop III supernovae (SNe) are trapped in the dense shells behind the forward shocks. Here we present the abundances of refractory elements in the dust-enriched SN shells, finding that the abundance patterns are in good agreement with that observed for a Galactic halo star, SDSS J102915+172927 (Caffau et al. 2011). On the other hand, our simple analysis of grain growth shows that the growth of dust can activate even for the metallicity as low as $Z = 10^{-5} Z_{\text{sun}}$ before dust emission cooling causes cloud-fragmentation. This implies that the grain growth could have potentials to affect the formation of the first low-mass stars.

Dust Evolution in Pop III SNe (Nozawa et al. 2007)

- Dust model: dust formed in the unmixed ejecta (Nozawa et al. 2003)
 - The fates of dust grains depend on their initial radii, a_{ini} (Figure 1)
 - $a_{\text{ini}} < 0.05 \mu\text{m}$: completely destroyed in the shocked hot gas
 - $0.05 \mu\text{m} < a_{\text{ini}} < 0.2 \mu\text{m}$: trapped in the shells behind the forward shocks
 - $a_{\text{ini}} > 0.2 \mu\text{m}$: injected into the ISM without being eroded significantly
- A part of newly formed grains is piled up in the dense SN shells !

Elemental abundances in the dust-enriched dense SN shells

Abundance patterns of C, O, Mg, and Si relative to Fe in the SN shells are in good agreement with that in SDSS J102915+17927 (Figure 2)

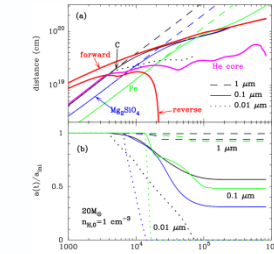


Fig. 1 – Time evolutions of (a) positions and (b) ratios of grain radii to the initial ones for a SNR model with $M_{\text{ZAMS}} = 20 M_{\odot}$ and $n_{\text{H},0} = 1.0 \text{ cm}^{-3}$. The trajectories of the forward and the reverse shocks are depicted by the thick red curves in (a). Dust species are C, MgSiO₃, and Fe with the initial radii of 0.01 μm (dotted), 0.1 μm (solid) and 1.0 μm (dashed).

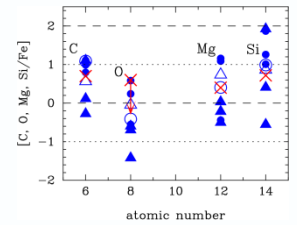


Fig. 2 – Abundances of C, O, Mg, and Si relative to Fe in the dense shells of Pop III SNRs with $M_{\text{ZAMS}} = 13, 20, 25,$ and $30 M_{\odot}$ for $n_{\text{H},0} = 0.1 \text{ cm}^{-3}$ (triangles) and $n_{\text{H},0} = 1.0 \text{ cm}^{-3}$ (circles). The abundance pattern of a halo star SDSS J102915+172927 ($Z = 4.5 \times 10^{-5} Z_{\odot}$) is plotted by the red crosses (Caffau et al. 2011). The open triangles and circles are, respectively, the results for $M_{\text{ZAMS}} = 30 M_{\odot}$ and $n_{\text{H},0} = 0.1 \text{ cm}^{-3}$, and $M_{\text{ZAMS}} = 25 M_{\odot}$ and $n_{\text{H},0} = 1.0 \text{ cm}^{-3}$, which show good agreements with the observed composition of SDSS J102915+172927.

Is grain growth possible in metal-poor star-forming clouds?

- Grain growth in dense clouds collapsing with the free-fall timescale
 - single-component dust, Fe and Si, with a single initial radius, $r_{i,0}$
 - initial dust abundance $f_{i,0}$ (number fraction of element i originally contained in dust)

Basic equations

mass conservation

$$f_i(t) = 1 - \frac{c_i^{\text{gas}}(t)}{c_i(t)} = f_{i,0} \left(\frac{r_i(t)}{r_{i,0}} \right)^3$$

growth rate of grain radius

$$\frac{dr_i}{dt} = s \left(\frac{4\pi}{3} a_{i,0}^3 \right) \left(\frac{kT_{\text{gas}}}{2\pi m_i} \right)^{1/2} c_i^{\text{gas}}(t)$$

- Results of calculations of grain growth (Figures 3 and 4)

- Grain growth is efficient even in the gas clouds with $[\text{Fe}, \text{Si}/\text{H}] \sim -5$
- For lower $[\text{X}/\text{H}]$ and lower $f_{i,0}$, grain growth proceeds at higher densities

Critical abundance and Dust-to-gas mass ratio

- Critical abundances, $A_{i,\text{crit}}$, above which grain growth becomes effective

$$A_{i,\text{crit}} = (1 - 2.5) \times 10^{-9} K_i \left(\frac{r_{i,0}}{0.01 \mu\text{m}} \right) \left(\frac{10^{12} \text{ cm}^{-3}}{c_{\text{H},*}} \right)^{1/2} \quad (\text{Figure 5})$$

where K_i is a function of $f_{i,0}$ and $f_{i,*}$ (initial and final condensation efficiencies)

- Dust-to-gas mass ratio corresponding to the critical abundance is well below the criterion for the dust-induced fragmentation (Figure 6)

- While, dust-to-gas mass ratio after grain growth can exceed this criteria

→ The increase of dust mass due to grain growth can cause the cloud-fragmentation as long as the above critical abundance is fulfilled

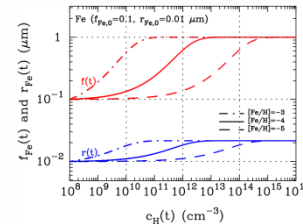


Fig. 3 – Time evolution of the condensation efficiency $f(t)$ (red) and grain radius $r(t)$ (blue) through the growth of Fe grains with the initial dust abundance $f_{\text{Fe},0} = 0.1$ and the initial grain radius $r_{\text{Fe},0} = 0.01 \mu\text{m}$ as a function of number density of hydrogen $c_{\text{H}}(t)$. Dot-dashed, solid, and dashed curves give the results for the collapsing clouds with the Fe abundance of $[\text{Fe}/\text{H}] = -3, -4,$ and -5 , respectively.

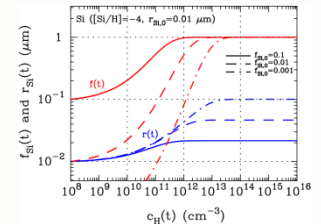


Fig. 4 – Time evolution of the condensation efficiency $f(t)$ (red) and grain radius $r(t)$ (blue) through the growth of Si grains of the initial radius $r_{\text{Si},0} = 0.01 \mu\text{m}$ in the collapsing cores with the Si abundance of $[\text{Si}/\text{H}] = -4$. Solid, dashed, and dot-dashed lines correspond to the results for the initial dust abundance of $f_{\text{Si},0} = 0.1, 0.01,$ and 0.001 , respectively.

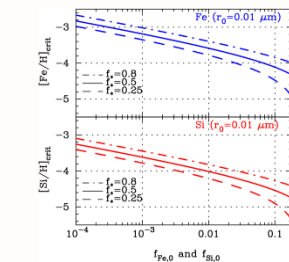


Fig. 5 – Critical abundances of Fe (upper) and Si (lower) above which the grain growth becomes effective before dust emission cooling causes the gas fragmentation, as a function of the initial dust abundance $f_{i,0}$. The initial grain radius is set as $r_{i,0} = 0.01 \mu\text{m}$. Dot-dashed, solid, and dashed curves give the abundances at which the condensation efficiency reaches $f_i^* = 0.6, 0.5,$ and 0.25 , respectively, at the density $c_{\text{H}} = 10^{12} \text{ cm}^{-3}$.

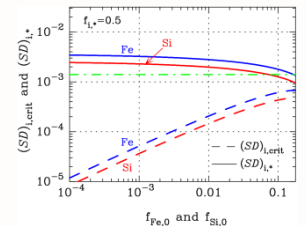


Fig. 6 – Products (SD)_{crit} and (SD)_{*} of dust-to-gas mass ratio D and cross section per unit dust mass S for Fe (blue) and Si (red) grains (red) as a function of the initial dust abundance $f_{i,0}$. Dashed lines depict (SD)_{crit} corresponding to the critical abundances given in Figure 5, whereas solid lines display (SD)_{*} when the condensation efficiency reaches $f_i^* = 0.5$ through the grain growth in dense clouds. The horizontal green dot-dashed line is the minimal criterion above which the dust cooling causes the fragmentation into low-mass clumps (Schneider et al. 2012a).

Discussion

- Abundance patterns of the SN shells enriched with SN dust match with that in SDSS J102915+17927

→ SDSS J102915+17927 might be the second-generation star formed in the dense shell of Pop III SN

- Even if the initial dust-to gas mass ratio is below the criterion for the dust-driven fragmentation, the grain growth increases the dust mass in dense clouds and can drive the formation of low-mass stars

→ It is not always required that a significant fraction of dust grains formed in SNe should survive

References:

Caffau, E., et al. 2011, Nature, 477, 67
 Nozawa, T., et al. 2003, ApJ, 598, 785
 Nozawa T., et al. 2007, ApJ, 666, 955
 Omukai, K. 2000, ApJ, 534, 809
 Omukai, K., et al. 2005, ApJ, 626, 627
 Schneider, R., et al. 2003, Nature, 422, 869
 Schneider, R., et al. 2006, MNRAS, 369, 1437
 Schneider, R., et al. 2012a, MNRAS, 419, 1566
 Schneider, R., et al. 2012b, MNRAS, (arXiv:1203.4234)